

Supplementary Materials for

Optimizing human apyrase to treat arterial thrombosis and limit reperfusion injury without increasing bleeding risk

Douglas Moeckel, Soon Soeg Jeong, Xiaofeng Sun, M. Johan Broekman, Annie Nguyen, Joan H. F. Drosopoulos, Aaron J. Marcus, Simon C. Robson, Ridong Chen,*
Dana Abendschein*

*Corresponding author. E-mail: rchen@apt-therapeutics.com (R.C.); dabendsc@DOM.wustl.edu (D.A.)

Published 6 August 2014, *Sci. Transl. Med.* **6**, 248ra105 (2014)
DOI: 10.1126/scitranslmed.3009246

The PDF file includes:

Materials and Methods

Fig. S1. Design of human ADPase-enhanced apyrases.

Fig. S2. Comparison of the enzymatic activities of APT102 and solCD39.

Fig. S3. Inhibition by APT102 of ADP-induced aggregation in human platelet-rich plasma.

Fig. S4. In vitro inhibition by APT102 of ADP-induced aggregation of rabbit, pig, and dog platelet-rich plasma.

Fig. S5. Effects of clopidogrel and prasugrel prodrugs on inhibition of ADP-induced aggregation of canine platelet-rich plasma achieved with recombinant solCD39 and APT102.

Fig. S6. Purification of APT102 from the supernatant of CHO cells stably transfected with the APT102 gene.

Fig. S7. Pharmacokinetics of APT102 in dogs.

Fig. S8. Pharmacodynamics of APT102 and clopidogrel in dogs.

Fig. S9. Experiment protocol for dogs undergoing coronary occlusion and fibrinolysis.

Fig. S10. Coronary artery blood flow in dogs before and after occlusion and fibrinolysis.

Fig. S11. Bleeding times in mice after clopidogrel with or without added APT102.

Table S1. Kinetic parameters of wild-type and mutant solCD39L3 and solCD39 toward ADP and ATP.

Table S2. In vitro inhibition of ADP-induced platelet aggregation with APT102.

Table S3. Coagulation parameters versus time after coronary occlusion and fibrinolysis in dogs.

Table S4. Hematologic values at baseline and 24 hours after coronary occlusion and fibrinolysis in individual dogs.

Table S5. Serum chemistry values at baseline and 24 hours after coronary occlusion and fibrinolysis in individual dogs.

References (49–51)

Materials and Methods

Sequence analysis and computer graphics

GenBank and Swiss-Prot databases were searched for amino acid sequence similarities using the BLAST and PSI-BLAST programs. Structure-based alignment was performed as follows: residues involved in binding and catalysis were identified from the X-ray crystal structure of rabbit actin. Other sequences were then aligned using active residues as key landmarks (32). GenBank/EMBL accession numbers are as follows: Rabbit actin, P68135; human actin, CAI19050; human HSP70, AAH36107; human CD39, AAB32152; human CD39L1, AAB81013; human CD39L2, AAC39883; human CD39L3, AAC39884; human CD39L4, AAC39885; human NTPDase4, Q9Y227. X-ray crystallographic structures were visualized with Swiss PDB Viewer. The coordinates of rabbit actin and its complexes with ADP or ATP were retrieved and transferred from Protein Data Bank (accession number 1ATN).

Gene cloning

The full-length cDNA sequence of CD39L3 was amplified from a human brain cDNA library (Clontech, Palo Alto, CA) using PCR and gene-specific primers and inserted into vector pGEM-T Easy (Invitrogen, Carlsbad, CA). A soluble form of CD39L3 (APT101) was generated by removing the N-terminal 44 amino acids and the C-terminal 43 amino acids. To facilitate subcloning into vectors suitable for expression in mammalian cells, a *Sma* I restriction site was created by PCR in frame with the ATG of APT101. The resulting PCR product was cloned into the *Sma* I site of pSP72 (Promega, Madison, WI). The full length cDNA for CD39 was isolated by PCR from a human placenta cDNA library (Clontech). Cloning and subcloning were performed following the same procedure as described for CD39L3. The wildtype and mutant genes of APT101 and solCD39 were cloned into expression plasmid pSEQTAG2a (Invitrogen), a vector

suitable for production of secreted recombinant protein in HEK 293T cells. To facilitate cloning, pSEQTAG2a was modified by site-directed mutagenesis (Quick Change, Stratagene, LaJolla, CA) to introduce a *Srf* I restriction site in frame with the Igκ leader sequence. The *Sma* I fragment of the genes was then translationally fused to the *Srf* I site. The GPEX vector was used for stable CHO cell expression, as described previously (38).

Site-Directed Mutagenesis

Point mutations were introduced using a mutagenesis kit (Stratagene) according to the manufacturer's instructions. Mutagenesis primers used to introduce the respective point mutations in solCD39 and APT101 are identified as follows:

5' -GGATGCCGGGTCTTCAGCGACCACAGTCTACGTG-3' APT101 R67A,

5' -GGATGCCGGGTCTTCAGGGACCACAGTCTACGTG-3' APT101 R67G,

5' -GCTGGATGCCGGGTCTTCAGCGACCCGCGTCTACGTGATCAATG-3' APT101 R67A/T69R,

5' -GCTGGATGCCGGGTCTTCAGGGACCCGCGTCTACGTGATCAATG-3' APT102,

5' -GTGCTGGATGCGGGTTCTTCTGGGACCGCTTATAACATCTATAAG-3' solCD39.

The entire open reading frame of the mutants generated was verified by DNA sequence analysis.

Protein expression and purification

Expression plasmids were transfected into 293T cell lines. Transiently transfected cells were selected in the presence of Zeocin (Invitrogen). Selected colonies were grown to full confluence and then inoculated into 15-30 ml of CD293 medium (Gibco) in a shaking flask (120 rpm) yielding about 5×10^5 cells/ml. Once fully adapted to serum-free suspension culture, stable APT102 cells were scaled up first in a 3 liter spinner flask, and then for large-scale production in 30 liter bioreactors as batch cultures with glucose and glutamine supplements. Bioreactor conditions were set at 37°C, 110 rpm and 5% CO₂. A typical 30 liter bioreactor was inoculated with 0.5×10^6

cells/ml and in 5 to 6 days HEK 293T cells typically grew to over 3.5×10^6 cells/ml. After removing the precipitate by centrifugation (12,000 x g for 30 min), conditioned medium was concentrated using an Amicon Stirrer and dialyzed against 100-fold volume of 10mM Tris (pH7.4). The protein preparation was applied to a DEAE Sepharose Fast Flow column (Amersham) and the enzyme fraction eluted with 10 mM Tris (pH7.4)/300 mM NaCl. Active fractions were identified with Malachite Green ADPase assay and concentrated using the Amicon Stirrer. Enzymes were then applied to a Heparin Sepharose column (Amersham) and washed with five column volumes of 10 mM Tris (pH7.4) and 10 mM Tris (pH7.4)/20 mM NaCl. Enzyme fractions were monitored by absorbance at 280 nm and identified with Malachite Green ADPase assay. Purity of recombinant proteins was determined with 4-12% Bis-Tris SDS NuPAGE gel (Invitrogen) and Coomassie Blue staining. Expression plasmids were stably transfected into CHO-S cell lines, as described previously (38). APT102 protein was purified in two steps with the use of anion exchange (ANX) and sulfopropyl (SP) columns (49) (fig. S6).

Apyrase assays and kinetic analysis

Spectrophotometric assays for ADPase and ATPase activities of apyrases were developed using Malachite Green as described (50). Briefly, following 30 minute incubation at 37°C, 50 μ l of the reaction solution was mixed with 900 μ l of 50 mM Tris-HCl (pH7.4)/8mM CaCl₂ and 50 μ l of malachite working solution. Inorganic phosphate release resulted in an increase of absorbance at 630 nm, monitored using an Agilent 8453 UV-Visible spectrophotometer (Agilent, Palo Alto, CA). In addition, radio-TLC assays for ADPase and ATPase activities were performed using [¹⁴C]ADP or [¹⁴C]ATP (NEN Life Science Products) following the procedure described previously for cell monolayers (33, 51). Radioactivity was quantitated with the use of a radio-TLC scanner (“InstantImager” Electronic Autoradiography System, Packard). Enzyme activity was corrected for

background activity (vector alone) and expressed as micromoles ADP or ATP per minute per milligram protein. Estimates of kinetic parameters were determined spectrophotometrically using unweighted nonlinear least-squares Newton-Raphson regressions to the Michaelis-Menten model.

***In vitro* platelet aggregation studies**

Blood was collected *via* 23 ga. butterfly needles from a peripheral vein of healthy animals and consenting human volunteers who had not ingested aspirin for at least one week. Anticoagulation was achieved with fresh acid citrate-dextrose (38 mM citric acid, 75 mM sodium citrate, 135 mM glucose) or heparin (100 U/ml). Platelet-rich plasma was obtained by centrifuging the blood at low speed (160 x g) for 10 minutes at room temperature. After the platelet-rich plasma was pipetted to a second tube, the remaining blood was centrifuged at high-speed (1,500 x g) for 50 minutes at room temperature to yield platelet-poor plasma. An aliquot of platelet-rich plasma (containing $1.0-1.2 \times 10^8$ platelets) was preincubated for 3 minutes at 37°C in an aggregometer cuvette (Lumiaggregometer) with added APT102 or isotonic Tris- buffered saline (Sigma, St. Louis, MO). Light absorption of plasma was controlled for by adding platelet-poor plasma and the total volume was adjusted to 300 μ l with Tris-buffered saline. After a 3 minute preincubation, ADP was added and the aggregation response was recorded for 4-6 minutes (33).

A

Enzyme	Specificity	ACR I	ACR IV
Rabbit actin	ATP	8 LVCD NG SGLVKAGFA	150 GIVL DSG DGVTHNVP
Human actin	ATP	8 LVCD NG SGLVKAGFA	150 GIVL DSG DGVTHNVP
Human HSP70	ATP	7 VGID L GTTYSVGVF	195 VLIF DL GGGTFDVSI
NTPDase1 (CD39)	ATP/ADP	58 IVL DAGSS H T S LYIY	216 FGAL DL GGASTQVTF
NTPDase2 (CD39L1)	ATP	42 IVL DAGSS H T SMFIY	197 LGAM DL GGASTQITF
NTPDase3 (CD39L3) [APT101]	ATP/ADP	59 IVL DAGSS R T T IVYVY	215 TGAL DL GGASTQISF
[APT102]	ADP/ATP	59 IVL DAGSS G T R VYVY	215 TGAL DL GGASTQISF
NTPDase4 (UDPase)	UDP	98 IVV DC GSSGSRVYVY	264 AGIL DM GGVSTQIAY
NTPDase5 (CD39L4)	UDP	51 IMF DAG STGTRIHVY	195 VGTL DL GGASTQITF
NTPDase6 (CD39L2)	UDP	104 IMF DAG STGTRVHVF	247 VGML DL GGG ST QIAF

B

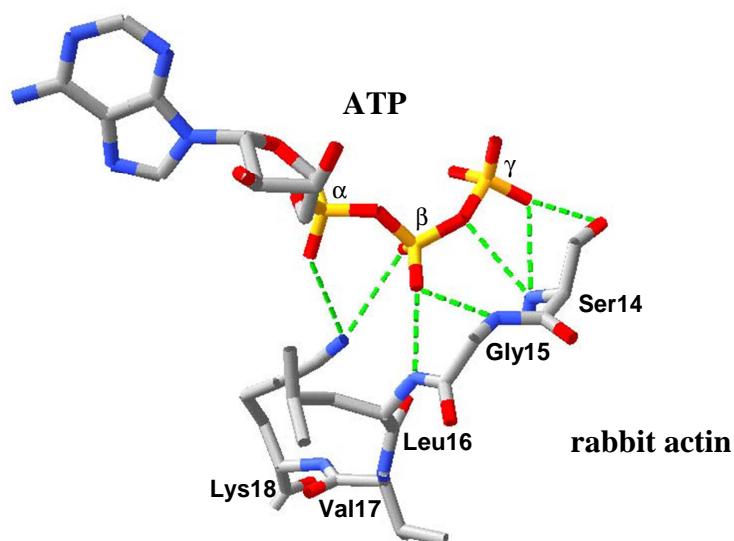


fig. S1. Design of human ADPase-enhanced apyrases. A). Alignment of human apyrase conserved regions I and IV (ACR I and ACR IV) to the actin/HSP70 superfamily. Sites subjected to mutagenesis are underlined and boldfaced; boldfaced text alone denotes strictly conserved amino acids. B). Rabbit actin (stick style model, 1ATN) interacting with α -, β - and γ -phosphates of ATP. Grey=carbon, blue=nitrogen, yellow=phosphate, red=oxygen. Hydrogen bonds are indicated by green dashed lines.

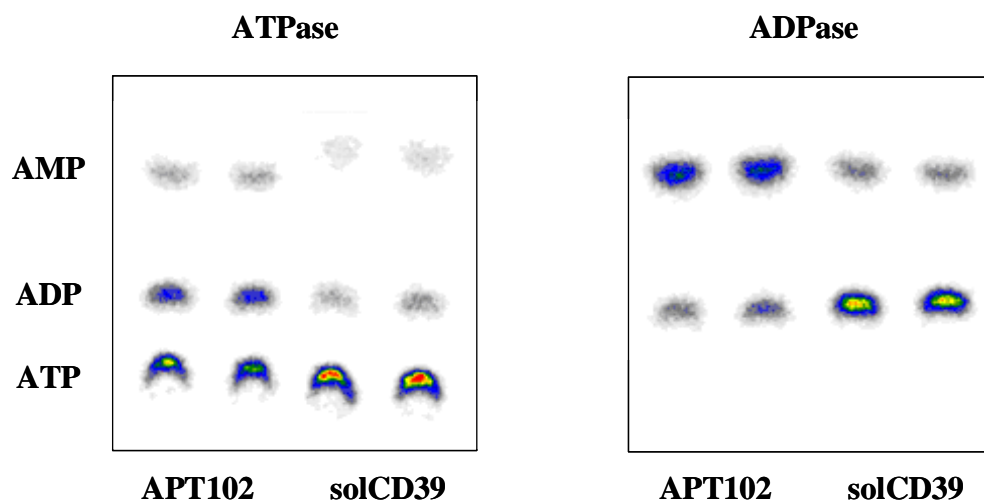


fig. S2. Comparison of the enzymatic activities of APT102 and solCD39. APT102 (2.7 ng) or solCD39 (2.9 ng) was incubated with [^{14}C]ATP (left panel) or [^{14}C]ADP (right panel). Radioactivity was quantitated by radio-TLC (thin-layer chromatography) scanning (red = highest radioactivity, blue/gray = lowest radioactivity). Results were calculated as averages of triplicate measurements following subtraction of buffer blanks.

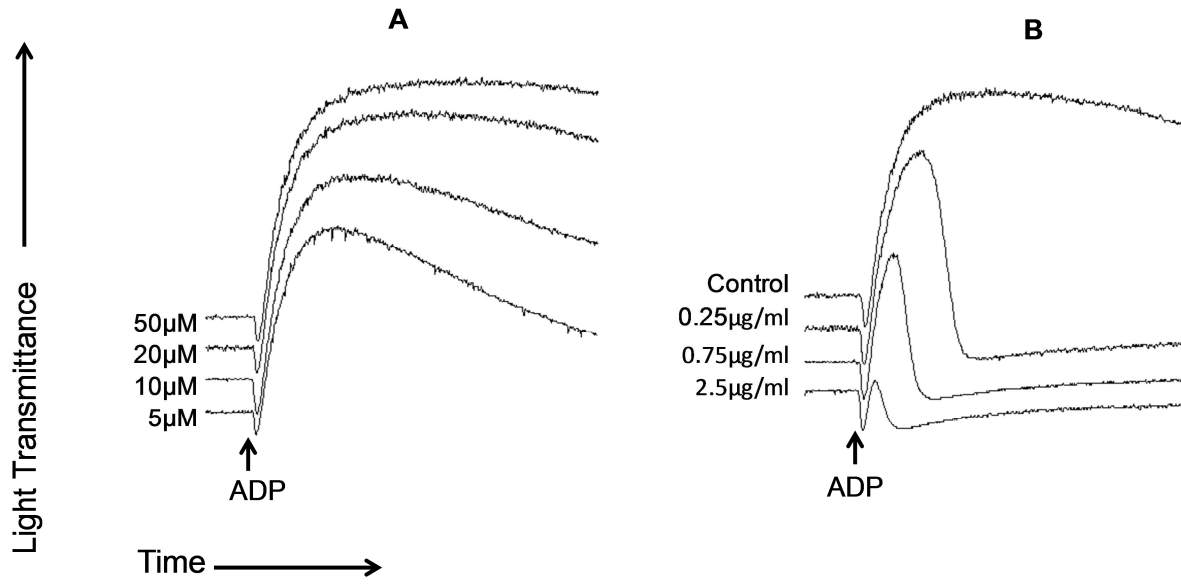


fig. S3. Inhibition by APT102 of ADP-induced aggregation in human platelet-rich plasma. A). Threshold-response to ADP confirming that $>5\mu\text{M}$ induces complete platelet aggregation. B). APT102 dose-dependently inhibited platelet aggregation induced by $20\mu\text{M}$ ADP added immediately after APT102. Blood was collected from a healthy human subject in tubes containing heparin (100U/ml) to maintain physiologic calcium concentration during the assay. Similar results were obtained in other healthy subjects.

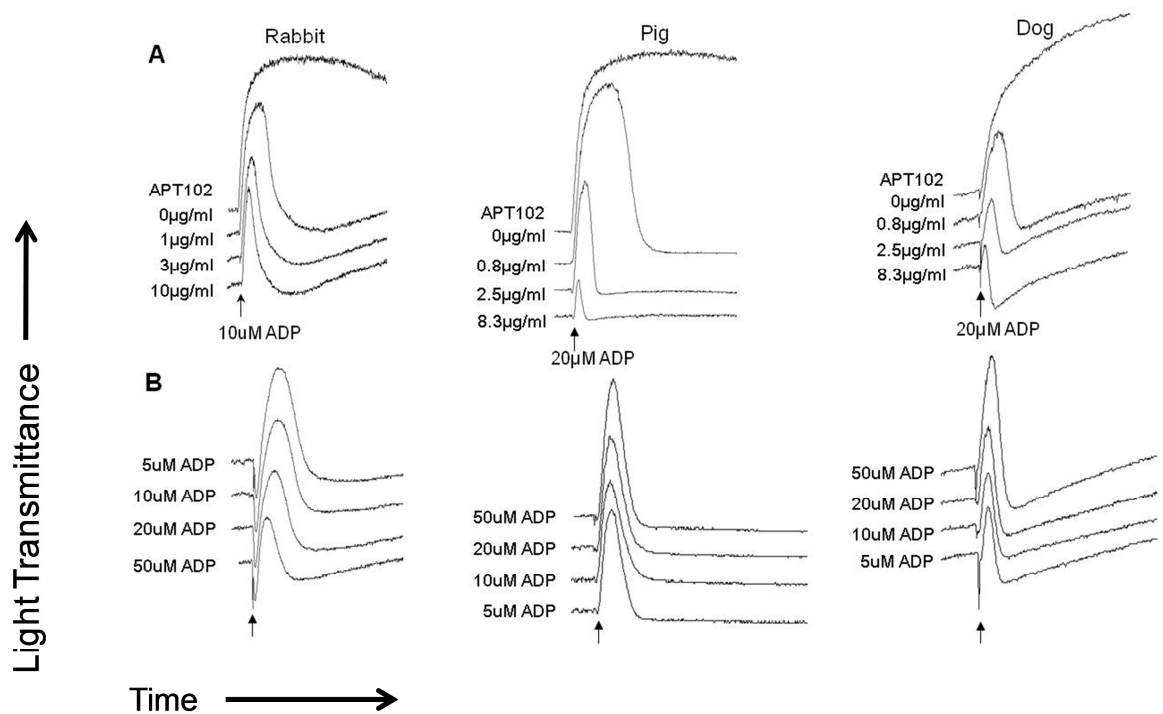


fig. S4. In vitro inhibition by APT102 of ADP-induced aggregation of rabbit, pig, and dog platelet-rich plasma. Blood samples were heparinized (100U/ml). **A).** APT102 dose- response. **B).** ADP-dose response with fixed APT102 concentration (2.5µg/ml). ADP was added at the arrows immediately after addition of APT102. Profiles are representative of triplicate measurements from at least three subjects.

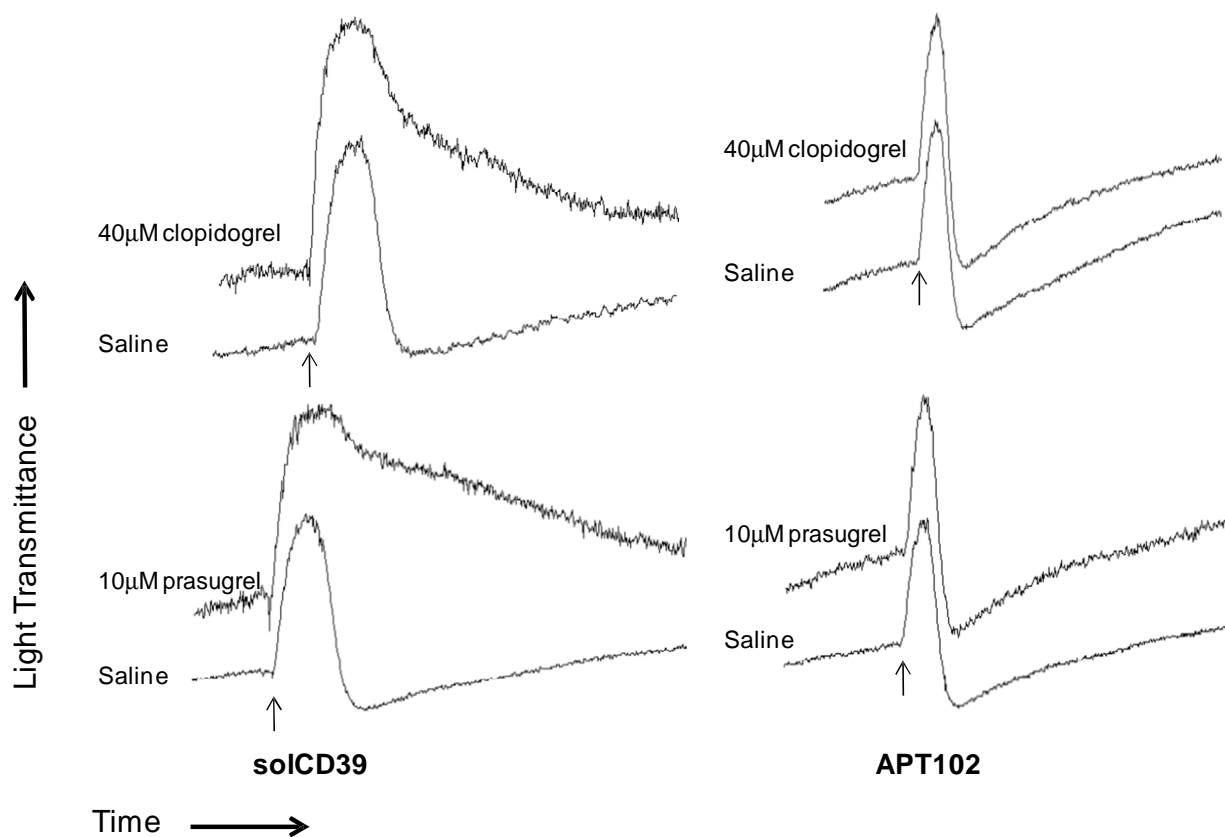


fig. S5. Effects of clopidogrel and prasugrel prodrugs on inhibition of ADP-induced aggregation of canine platelet-rich plasma achieved with recombinant solCD39 and APT102. Pre-incubation of platelet-rich plasma with typical loading doses of clopidogrel (40 μ M) or prasugrel (10 μ M) reduced the ability of solCD39 (left) to block ADP- induced aggregation but did not alter the inhibitory effect of APT102 (right). Aggregation was induced with 20 μ M ADP added immediately after the apyrase (arrows).

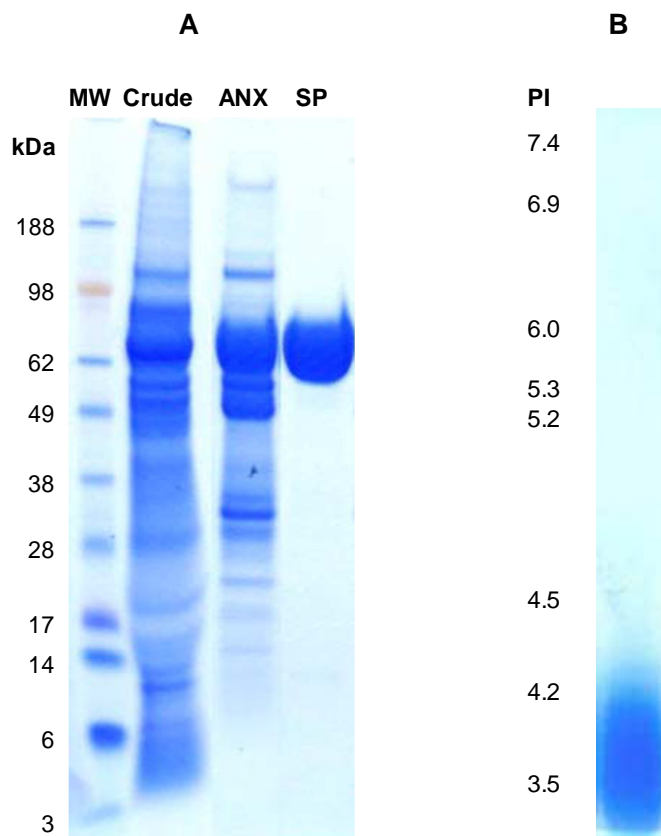


fig. S6. Purification of APT102 from the supernatant of CHO cells stably transfected with the APT102 gene. (A) Proteins (20 μ g) were separated on 10% SDS-PAGE after purification on ANX and SP columns. The single band at 65kD in the right lane (SP) is the purified APT102. (B) Isoelectric focusing gel showing the pI of APT102 at 3.0-4.0.

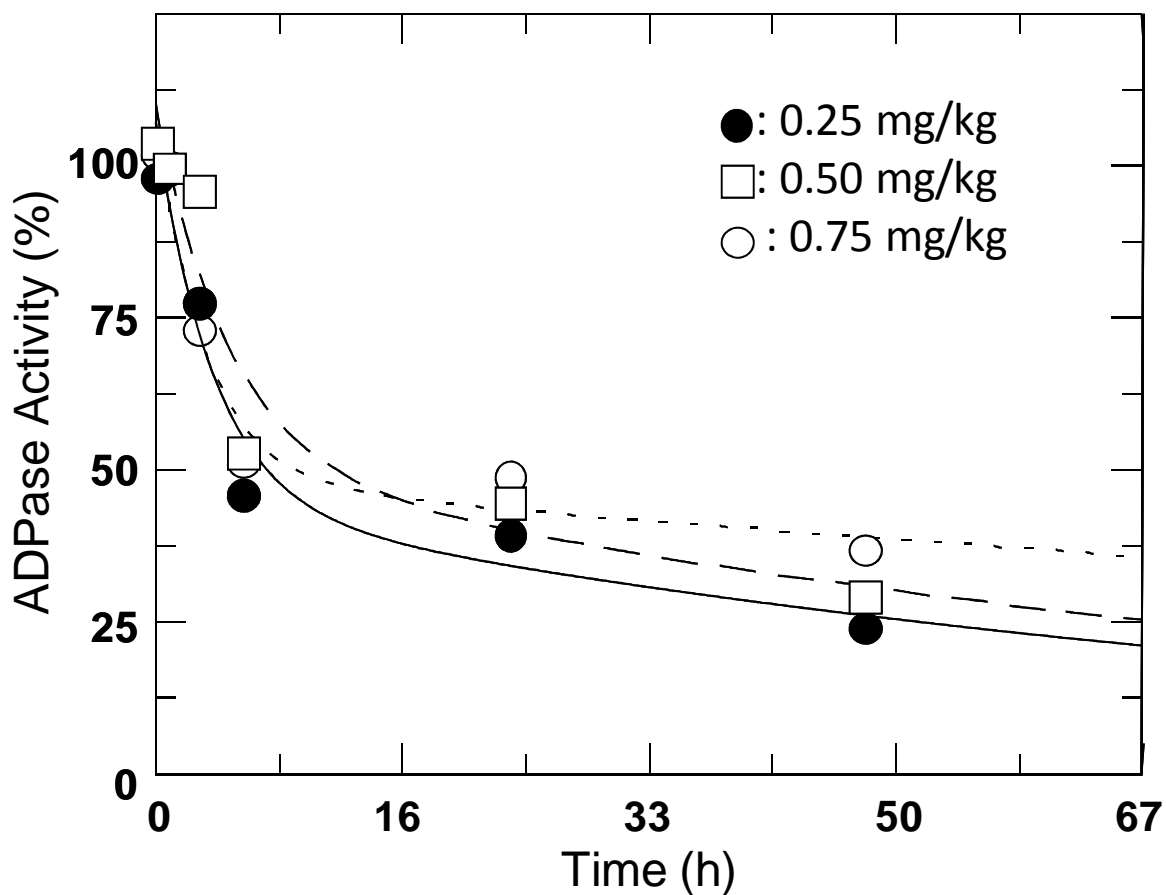


fig. S7. Pharmacokinetics of APT102 in dogs. APT102 was injected intravenously as a single bolus dose at time = 0 (n=2 for 0.25 and 0.5 mg/kg and n=1 for 0.75 mg/kg). Blood samples were collected in heparin, and ADPase activity was assayed in triplicate with a spectrophotometric method. Each data point represents the average of triplicate assays of ADPase activity at the given time point after APT102 injection.

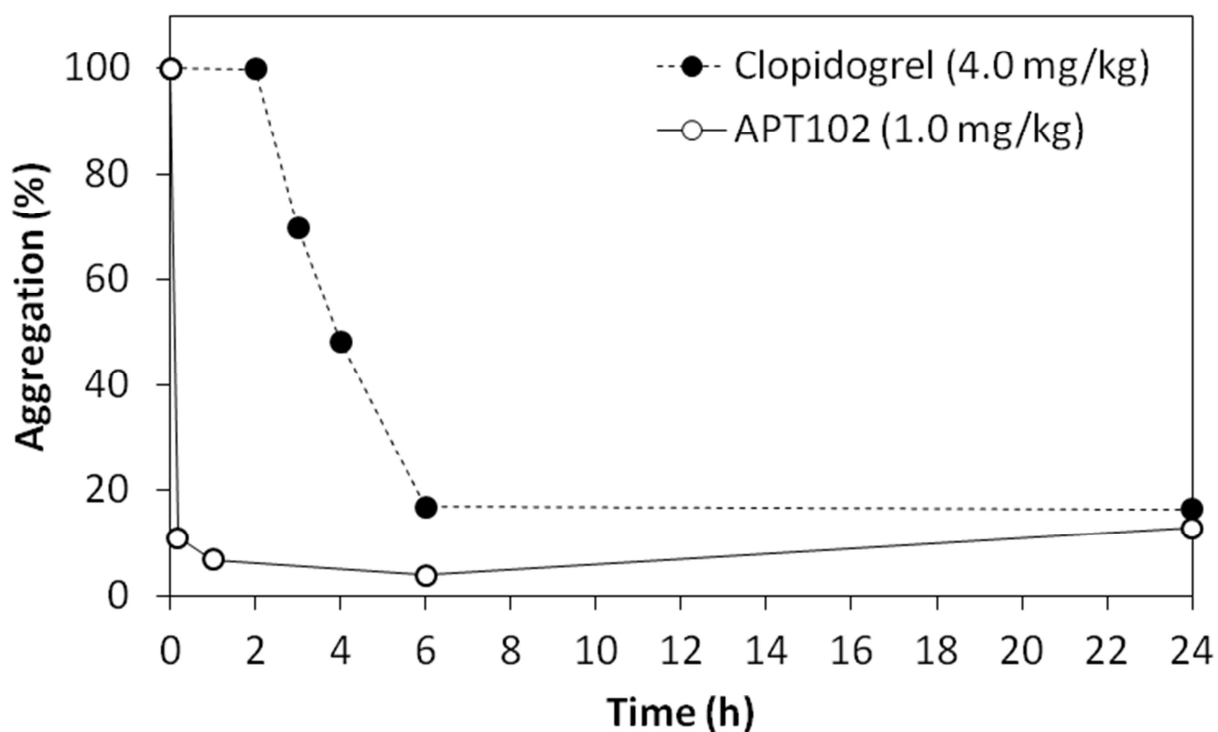


fig. S8. Pharmacodynamics of APT102 and clopidogrel in dogs. Platelet-rich plasma was obtained before ($t = 0$) and serially after either IV injection of APT102 (1.0 mg/kg, $n=2$) or oral administration of clopidogrel (4.0 mg/kg, $n=2$ dogs) in dogs. Aggregation of heparinized platelet-rich plasma was induced with 20 μ M ADP and monitored turbidimetrically. Inhibition of aggregation with clopidogrel was delayed because the pro-drug must be metabolized by P450 enzymes in the liver to the active inhibitor of P2Y₁₂ receptors. Results are the average of two dogs expressed as a percentage of the baseline aggregation.

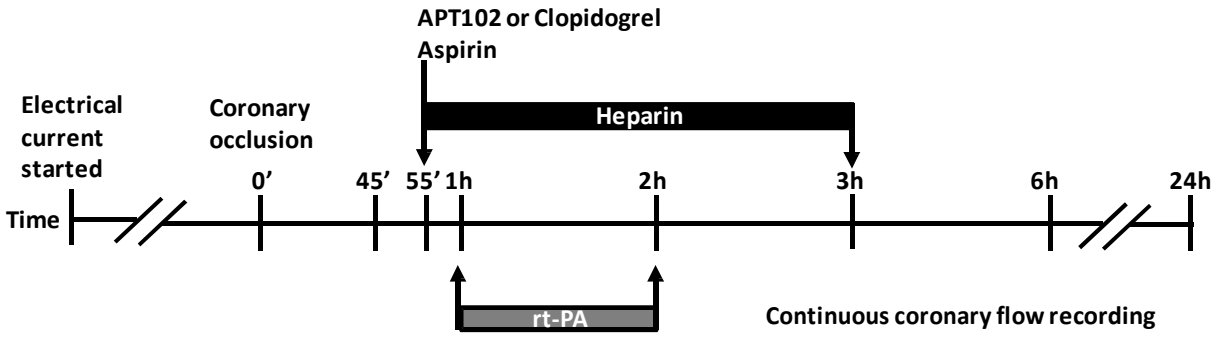


fig. S9. Experiment protocol for dogs undergoing coronary occlusion and fibrinolysis. Time 0 equals coronary occlusion indicated by zero coronary flow. Blood samples were collected and bleeding times were measured 45 minutes after coronary occlusion, and 3, 6, and 24 hours after coronary occlusion. rt-PA= human recombinant tissue-type plasminogen activator.

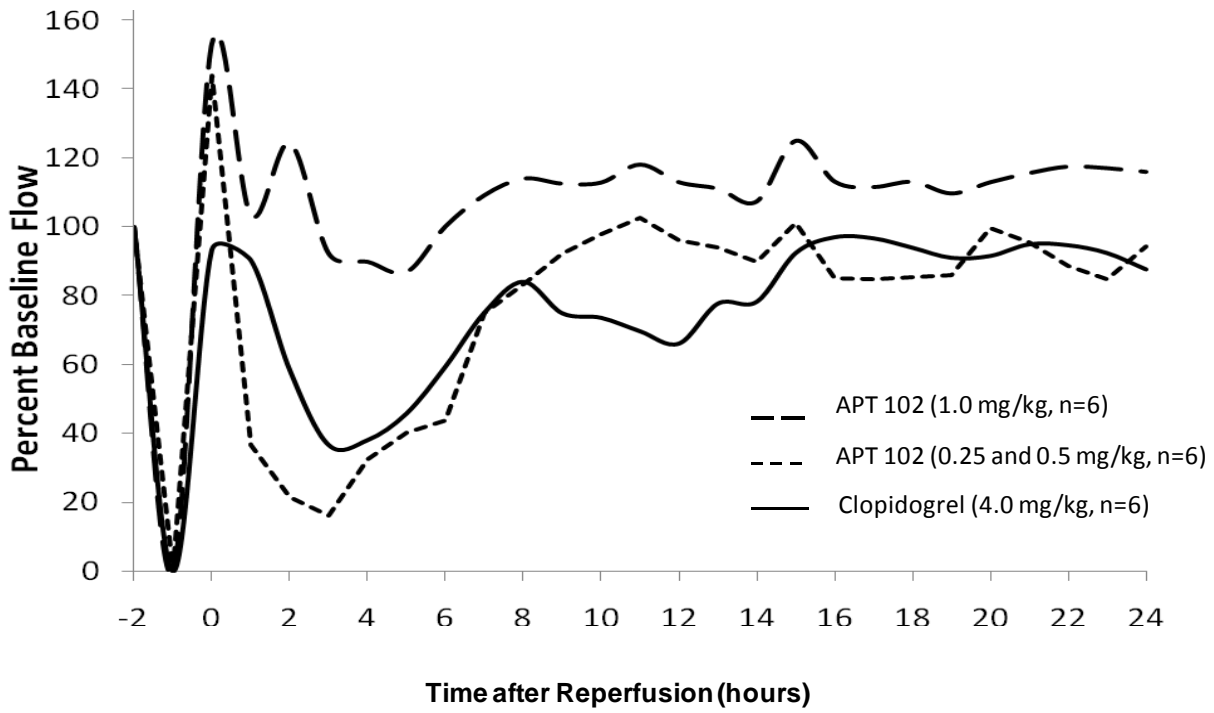


fig. S10. Coronary artery blood flow in dogs before and after occlusion and fibrinolysis. The rate is expressed as a percentage of the baseline values versus time after rt-PA-induced reperfusion ($t=0$) in dogs. Blood flow was measured with an electromagnetic flow probe placed around the coronary artery during surgery 1 week previously. All doses of APT102 caused hyperemic flow after reperfusion. The high dose of APT102 maintained coronary flow mostly above baseline (100%) during reperfusion, whereas the low dose of APT102 and clopidogrel treatment resulted in reocclusion in all dogs and flow did not return to baseline during 24 hours.

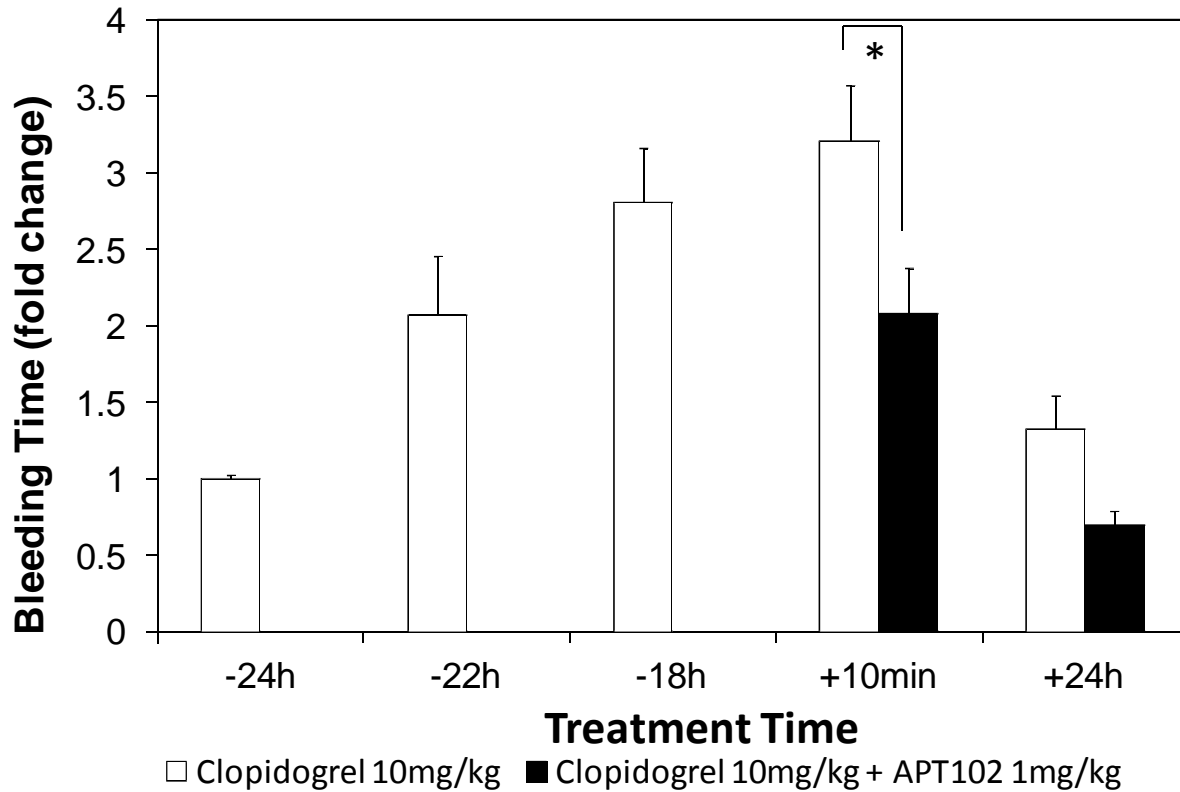


fig. S11. Bleeding times in mice after clopidogrel with or without added APT102. Clopidogrel was administered (PO) after the baseline sample (-24h). Bleeding times were measured 2 hours (-22 h) and 6 hours (-18 h) after clopidogrel administration (n=10 animals) and 10 minutes and 24 hours after IV APT102 administration (n=7 animals). Bars represent the mean \pm SEM. *p<0.05 compared with baseline by t test.

table S1. Kinetic parameters of wild-type and mutant solCD39L3 and solCD39 toward ADP and ATP.

Enzyme	ADP			ATP			Preference ¹ ADPase/ATPase	Preference ² ADPase/ATPase
	K_m μM	k_{cat} sec^{-1}	Performance k_{cat}/K_m $\mu\text{M}^{-1}\text{sec}^{-1}$	K_m μM	k_{cat} sec^{-1}	Performance k_{cat}/K_m $\mu\text{M}^{-1}\text{sec}^{-1}$		
SolCD39L3								
Wild type (APT101)	134.09	151.87	1.13	135.93	458.86	3.38	0.34	0.58
R67A	257.00	160.60	0.62	257.00	338.82	1.32	0.47	
R67G	281.80	183.50	0.65	152.90	327.28	2.14	0.30	
R67A/T69R	27.00	143.09	5.30	10.00	143.09	14.31	0.37	
R67G/T69R (APT102)	46.42	203.44	4.38	29.09	155.10	5.33	0.82	2.04
SolCD39								
Wild type	11.00	11.27	1.02	3.48	7.99	2.30	0.45	1.20
H66G/S68R	35.00	45.62	1.30	45.87	77.52	1.69	0.77	

¹ Spectrophotometric assay² Radio-TLC assay

All standard errors are <15% of the estimates

table S2. In vitro inhibition of ADP-induced platelet aggregation with APT102. Blood samples were collected in heparin. Aggregation of platelets in platelet-rich plasma was induced with 20 μ M ADP. The data were generated from triplicate measurements of each sample. Values represent means \pm SEM.

Species (n)	Anticoagulant	ADP	EC₅₀ (μg/ml)
Human (2)	Heparin	20 μ M	0.09 \pm 0.02
Rat (6)	Heparin	20 μ M	0.29 \pm 0.02
Rabbit (2)	Heparin	20 μ M	0.11 \pm 0.03
Pig (2)	Heparin	20 μ M	0.65 \pm 0.02
Dog (4)	Heparin	20 μ M	0.37 \pm 0.01

table S3. Coagulation parameters versus time after coronary occlusion and fibrinolysis in dogs. The animals were given either clopidogrel or APT102. Values represent mean \pm SD. * $p < 0.05$ compared with baseline by General Linear Models Repeated Measures ANOVA.

PT (sec)	Baseline	3h	6h	24h
Clopidogrel (4.0 mg/kg, n=6)	7.3 \pm 0.4	8.0 \pm 0.9	7.7 \pm 0.6	7.3 \pm 0.6
APT 102 (low dose, n=6)	8.1 \pm 0.5	7.9 \pm 0.3	8.2 \pm 0.2	7.7 \pm 0.8
APT 102 (1.0 mg/kg, n=6)	7.0 \pm 0.3	7.9 \pm 0.5	7.8 \pm 0.5	7.8 \pm 1.4
aPTT (sec)	Baseline	3h	6h	24h
Clopidogrel (4.0 mg/kg, n=6)	8.3 \pm 1.0	20.7 \pm 9.6*	13.9 \pm 4.4*	12.9 \pm 5.3
APT 102 (low dose, n=6)	8.5 \pm 1.0	17.1 \pm 2.7*	13.8 \pm 7.9*	17.9 \pm 17.1
APT 102 (1.0 mg/kg, n=6)	9.0 \pm 1.1	24.2 \pm 9.3*	19.5 \pm 13.7*	12.9 \pm 4.4

table S4. Hematologic values at baseline and 24 hours after coronary occlusion and fibrinolysis in individual dogs. The animals were given either clopidogrel or APT102. Group values represent means \pm SD. Statistical analyses were performed using General Linear Models Repeated Measures ANOVA. *Range of normal values in the canine (from Iowa State database); †= p<0.008; ‡=p<0.04 vs baseline.

Treatment	PLT (ths/mm ³)		RBC (mil/mm ³)		Hgb (g/dL)		PCV (%)	
	BSLN	24 h	BSLN	24 h	BSLN	24 h	BSLN	24 h
Clopidogrel	178	240	7.7	5.2	15.8	10.4	53.2	35.4
	274	291	6.4	4.1	13.8	8.1	46.7	29.1
	238	300	5.9	6.4	12.3	12.8	37.6	41.3
	219	-	7.5	-	16.7	-	49.9	-
	377	326	6.5	3.7	13.2	7.8	41.4	24.6
	377	391	6.3	4.6	13.1	9.1	40.3	29.0
MEAN \pm STD DEV	277 \pm 83	310 \pm 55	6.7 \pm 0.7	4.8 \pm 1.1†	14.2 \pm 1.7	9.6 \pm 2.0†	44.9 \pm 6.1	31.9 \pm 6.5‡
APT102 0.25 mg/kg	251	245	7.9	7.0	17.8	16.5	54.6	47.7
	297	270	5.7	4.7	11.4	10.4	35.6	29.3
	224	254	6.6	6.7	13.8	13.7	42.0	43.0
MEAN \pm STD DEV	257 \pm 37	256 \pm 13	6.7 \pm 1.1	6.1 \pm 1.3	14.3 \pm 3.2	13.5 \pm 3.0	44.1 \pm 9.7	40.0 \pm 9.6
APT102 0.5 mg/kg	336	227	5.0	2.4	10.2	4.6	32.5	15.1
	143	314	5.3	5.4	11.0	11.5	34.7	35.2
	96	218	6.8	5.2	15.2	10.9	49.3	36.8
MEAN \pm STD DEV	192 \pm 127	253 \pm 53	5.7 \pm 1.0	4.3 \pm 1.7	12.1 \pm 2.7	9.0 \pm 3.8	38.8 \pm 9.1	29.0 \pm 12.1
Total Low Dose Mean \pm SD	225 \pm 91	255 \pm 35	6.2 \pm 1.1	5.2 \pm 1.7	13.2 \pm 2.9	11.3 \pm 4.0	41.5 \pm 8.9	34.5 \pm 11.5
APT102 1.0 mg/kg	370	297	6.3	5.2	13.9	11.4	40.1	32.1
	292	329	6.4	6.7	14.1	14.7	42.1	44.6
	393	297	6.9	5.4	15.7	11.5	45.7	35.0
	405	338	6.4	5.3	14.1	11.1	33.6	24.6
	269	237	7.2	5.4	15.4	11.6	46.4	34.5
	305	266	5.7	4.2	13.2	9.2	39.5	28.5
MEAN \pm STD DEV	339 \pm 57	294 \pm 38	6.5 \pm 0.5	5.4 \pm 0.8‡	14.4 \pm 1.0	11.6 \pm 1.8‡	41.2 \pm 4.7	33.2 \pm 6.8‡

table S5. Serum chemistry values at baseline and 24 hours after coronary occlusion and fibrinolysis in individual dogs. The animals were given either clopidogrel or APT102. Values represent means \pm SD. Statistical analyses were performed using General Linear Models Repeated Measures ANOVA. .*Range of normal values in the canine (from Iowa State database).

Treatment	BUN (mg/dL)		Creat (mg/dl)		AST (U/L)		ALT (U/L)		Alk Phos (U/L)	
	BSLN	(7-24 mg/dl)* 24 h	BSLN	(0.7-1.4 mg/dl)* 24 h	BSLN	(<105 U/L)* 24 h	BSLN	(4-90 U/L)* 24 h	BSLN	(3-70 U/L)* 24 h
Clopidogrel 4.0mg/kg	13	15	0.9	1.0	98	71	185	142	-	201
	8	10	0.8	0.6	36	201	66	115	185	115
	10	12	0.7	0.8	36	96	49	79	83	77
	18	-	0.7	-	62	-	77	-	67	-
	7	34	0.7	1.0	81	619	74	109	99	116
	15	13	0.6	0.6	62	281	66	140	87	61
MEAN \pm STD DEV	12 \pm 4	17 \pm 10	0.7 \pm 0.1	0.8 \pm 0.2	63 \pm 25	254 \pm 221	86 \pm 49	117 \pm 26	104 \pm 47	114 \pm 54
APT102 0.25 mg/kg	9	15	0.7	0.8	24	73	66	80	157	81
	14	9	0.7	0.7	48	36	94	73	81	89
	14	12	0.8	0.7	40	120	75	134	52	46
MEAN \pm STD DEV	12 \pm 3	12 \pm 3	0.7 \pm 0.1	0.7 \pm 0.1	37 \pm 12	76 \pm 42	78 \pm 14	96 \pm 33	97 \pm 54	72 \pm 23
APT102 0.5 mg/kg	9	12	0.5	0.5	80	159	107	86	-	50
	11	11	0.7	0.8	70	542	95	161	96	103
	13	11	0.9	0.8	39	105	74	86	172	111
MEAN \pm STD DEV	11 \pm 2	11 \pm 0.6	0.7 \pm 0.2	0.7 \pm 0.2	63 \pm 21	269 \pm 238	92 \pm 17	111 \pm 43	134	88 \pm 33
Total Low Dose Mean \pm SD	12 \pm 2	12 \pm 2	0.7 \pm 0.1	0.7 \pm 0.1	50 \pm 21	173 \pm 186	85 \pm 16	103 \pm 36	112 \pm 51	80 \pm 27
APT102 1.0mg/kg	12	15	0.6	0.8	17	33	53	43	105	82
	11	11	0.7	0.8	40	41	60	53	116	103
	24	25	0.6	0.8	56	51	130	81	92	74
	16	14	0.6	0.7	52	120	53	72	103	80
	16	10	0.6	0.5	152	542	160	158	39	43
	15	11	0.6	0.5	172	285	172	158	144	90
MEAN \pm STD DEV	16 \pm 5	14 \pm 6	0.6 \pm 0.04	0.7 \pm 0.1	82 \pm 64	179 \pm 202	105 \pm 56	94 \pm 51	100 \pm 35	79 \pm 20